# Analysis of the spin exchange interactions of ferromagnetic $CdVO_3$ in terms of first principles and qualitative electronic structure calculations

D. Dai, H.-J. Koo, and M.-H. Whangbo[*]

*Department of Chemistry, North Carolina State University, Raleigh, NC 27695-8204, USA*

Received 6 February 2003; received in revised form 10 May 2003; accepted 20 May 2003

## Abstract

First principles spin-polarized electronic band structure calculations were carried out for three ordered spin states of $CdVO_3$, and the strengths of its corner- and edge-sharing spin exchange interactions were estimated. To gain insight into why $CdVO_3$ exhibits ferromagnetism while $CaV_2O_5$ does not despite their apparent structural similarity, the spin exchange interactions of $CdVO_3$ and $CaV_2O_5$ were compared in terms of spin dimer analysis using extended Hückel tight binding calculations, and the local geometries of their $V^{4+}$ ions were examined.

© 2003 Elsevier Inc. All rights reserved.

## 1. Introduction

The $CdVO_3$ phase had been known for some time [1–3] before its precise crystal structure and magnetic properties were determined a few years ago [4]. The magnetic susceptibility data of $CdVO_3$ collected from 77 to 297 K were found to exhibit a Curie–Weiss behavior with a positive Weiss temperature hence hinting the presence of ferromagnetism [3]. That $CdVO_3$ is indeed ferromagnetic was proven unambiguously by the magnetization and electron paramagnetic resonance studies of Onoda and Nishiguchi [4]. $CdVO_3$ consists of isolated $VO_3$ chains made up of corner- and edge-sharing $VO_5$ square pyramids (Figs. 1a and b). The $V^{4+}$ ($d^1$) ions of each $VO_3$ chain form a zigzag chain (Fig. 1c), and adjacent $V^{4+}$ ions interact through corner-sharing ($J_c$) and edge-sharing ($J_e$) exchange paths. It was found [4] that the magnetic susceptibility of $CdVO_3$ above 50 K is well described by the spin-1/2 ferromagnetic Heisenberg model [5] with one exchange parameter $J = 8.6$ meV. This finding, together with the qualitative observation [6] that an edge-sharing spin exchange between first-row metal ions can be ferromagnetic when the direct overlap between their $3d$ orbitals is weak, led Onoda and Nishiguchi to suggest that $J_e$ is ferromagnetic and $J_c$ is significantly weaker in strength than $J_e$ [4].

The occurrence of ferromagnetism in $CdVO_3$ is quite intriguing because it is typically antiferromagnetism that is found in magnetic oxides made up of $VO_5$ square pyramids containing $V^{4+}$ ions. Representative examples include $AV_2O_5$ ($A$ = Ca, Mg) [7–12] and $AV_4O_9$ ($Cs_2$, Ca, Sr, $H_2N(CH_2CH_2)_2NH_2$) [12–18]. In particular, the $VO_5$ square pyramid and the zigzag $V^{4+}$ chain unit of $CdVO_3$ are very similar in structure to those of $CaV_2O_5$. The $V_2O_5$ layers of $CaV_2O_5$ are made up of corner-sharing $VO_3$ chains such that the $V^{4+}$ ions between adjacent $VO_3$ chains interact through corner-sharing exchange paths $J_c'$ (Fig. 1d). In the present work, we estimate quantitatively the spin exchange parameters $J_e$ and $J_c$ of $CdVO_3$ using first principles spin-polarized electronic band structure calculations. Then we probe why ferromagnetic interactions dominate in $CdVO_3$ but antiferromagnetic interactions do in $CaV_2O_5$ by analyzing the edge- and corner-sharing spin exchange interactions of $CdVO_3$ and $CaV_2O_5$ on the basis of tight binding electronic structure calculations and then comparing the local geometries of their $V^{4+}$ ions.

## 2. Mapping analysis of spin exchange interactions

Spin exchange parameters of an extended magnetic solid can be quantitatively determined on the basis of first principles electronic structure calculations using the
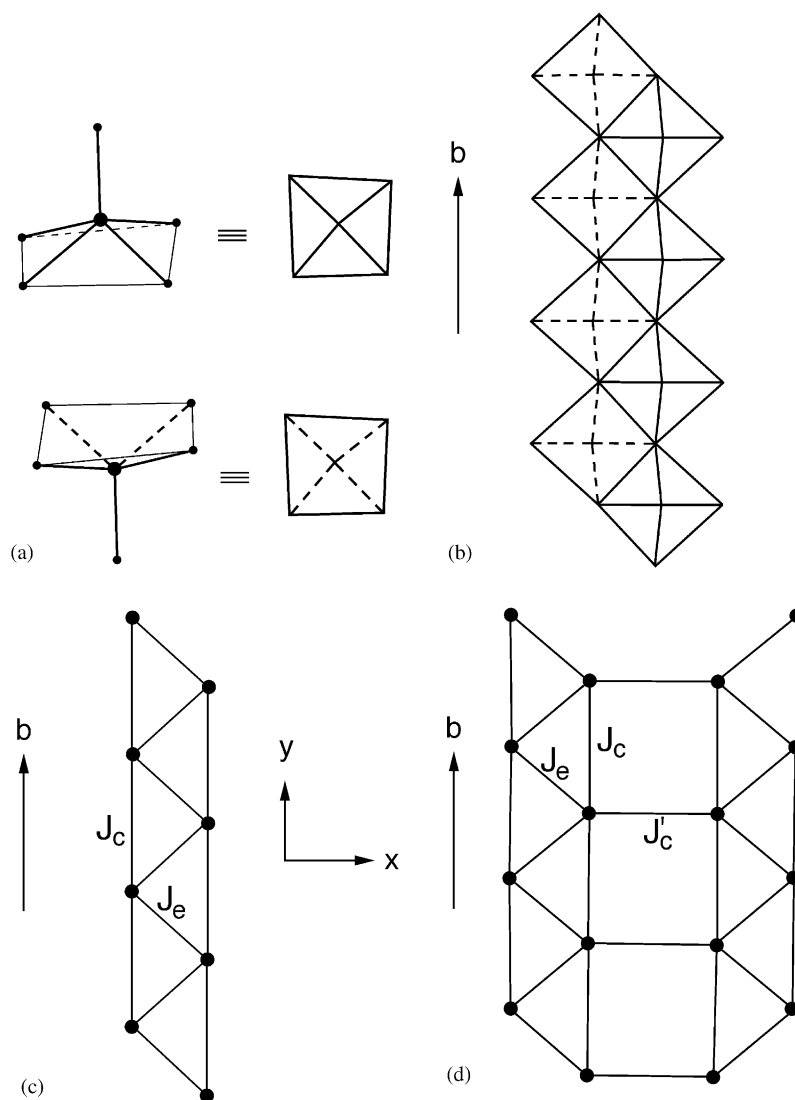
---

Fig. 1. (a) Representations of $VO_5$ square pyramids with the apical oxygen atom lying above and below the $O_4$ basal plane. (b) Schematic projection view of a $VO_3$ chain of $CdVO_3$. (c) Arrangement of the $V^{4+}$ ions (represented by dots) in a $VO_3$ chain of $CdVO_3$. (d) Arrangement of the $V^{4+}$ ions (represented by dots) in a $V_2O_5$ layer of $CaV_2O_5$.

"mapping" [19–21] or "direct" method [11, 22]. In the mapping method, the energies of several electronic states of a magnetic solid (or its fragments) are determined by electronic structure calculations, and then the energy differences between these electronic states are mapped onto those between the corresponding spin states determined by an appropriate spin Hamiltonian. In the direct method, spin exchange parameters of a magnetic solid are directly calculated from its ground state electronic structure on the basis of electronic band structure calculations.

In the cluster approach to the mapping analysis [19], one defines the spin dimer for each exchange path as the structural fragment containing the two interacting spin sites. Then the energies of two different electronic states of the spin dimer are determined by first principles

electronic structure calculations, and the corresponding spin states are generated by employing either a Heisenberg or an Ising Hamiltonian depending upon the nature of electronic structure calculations employed [20]. In the noncluster approach to the mapping analysis [21], the electronic energies of a magnetic solid are determined for a number of states with ordered spin arrangements on the basis of spin-polarized electronic band structure calculations, and the corresponding spin states are generated in terms of an Ising Hamiltonian. In the present work, this latter method was employed to evaluate the $J_c$ and $J_e$ values of $CdVO_3$.

To determine the two spin exchange parameters $J_c$ and $J_e$ of $CdVO_3$ (Fig. 1d), we consider the three ordered spin states $|HS\rangle$, $|BS_1\rangle$, and $|BS_2\rangle$, depicted in Fig. 2. In general, the Ising Hamiltonian for an extended

solid is written as

$$\hat{H}^{\text{Ising}} = -\sum_{ij} J_{ij} \hat{S}_{iz} \hat{S}_{jz}. \qquad (1)$$

Thus, for an isolated zigzag chain of $CdVO_3$, the energies of the three spin states per formula unit (FU) (i.e., per spin site) are written as

$$E(\text{HS}) = \langle \text{HS}|\hat{H}^{\text{Ising}}|\text{HS} \rangle = -\frac{1}{4}J_e - \frac{1}{4}J_c, \qquad (2a)$$

$$E(\text{BS}_1) = \langle \text{BS}_1|\hat{H}^{\text{Ising}}|\text{BS}_1 \rangle = \frac{1}{4}J_e - \frac{1}{4}J_c, \qquad (2b)$$

$$E(\text{BS}_2) = \langle \text{BS}_2|\hat{H}^{\text{Ising}}|\text{BS}_2 \rangle = \frac{1}{4}J_c. \qquad (2c)$$

Consequently, the spin exchange parameter $J_e$ is related to the state energy difference as

$$J_e = 2[E(\text{BS}_1) - E(\text{HS})]. \qquad (3a)$$

Then, the spin exchange parameter $J_c$ is obtained either as

$$J_c = \frac{1}{2}J_e - 2[E(\text{BS}_1) - E(\text{BS}_2)] \qquad (3b)$$

or as

$$J_c = \frac{1}{2}J_e + 2[E(\text{BS}_2) - E(\text{HS})]. \qquad (3c)$$

Therefore, the $J_c$ and $J_e$ values are determined when the energies (per FU) of the electronic states corresponding to the spin states $|\text{HS} \rangle$, $|\text{BS}_1 \rangle$ and $|\text{BS}_2 \rangle$, are obtained by first principles electronic band structure calculations.

## 3. First principles electronic structure calculations and spin exchange parameters

To determine the electronic energies of the three ordered spin states, $|\text{HS} \rangle$, $|\text{BS}_1 \rangle$ and $|\text{BS}_2 \rangle$, we carried out spin-polarized first principles full potential linearized plane wave (FP-LAPW) calculations using the WIEN2k program package [23] with the generalized gradient approximation [24] for the exchange-correlation energy. Both ferromagnetic and anti-ferromagnetic calculations were performed with the $(a, 2b, c)$ supercell. We employed the muffin-tin radii of 2.57 au for Cd, 1.59 au for V, and 1.56 au for O. The basis set cut-off parameters were $G_{\text{max}} = 14$ and $R_{\text{mt}}K_{\text{max}} = 7$. Integrations over the irreducible wedge of the Brillouin zone were performed using a 40 k-point regular mesh. Results of our calculations are summarized in Tables 1, 2 and Figs. 3–5.

The present FP-LAPW calculations show that the $|\text{HS} \rangle$ state of $CdVO_3$ is more stable than the



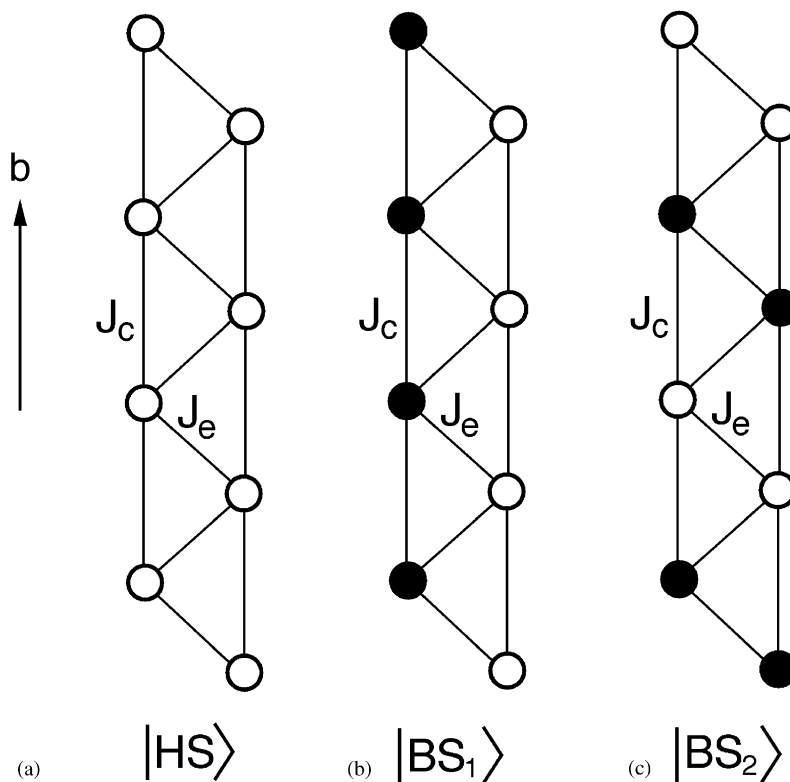Fig. 2. Three ordered spin arrangements in an isolated $VO_3$ chain of $CdVO_3$. (a) Ferromagnetic arrangement $|\text{HS} \rangle$. (b) Antiferromagnetic arrangement $|\text{BS}_1 \rangle$. (c) Antiferromagnetic arrangement $|\text{BS}_2 \rangle$. Here the labels "HS" and "BS" refer to "highest-spin" and "broken-symmetry", respectively.

Table 1
Electronic energies $E$ (Ryd/FU) and relative energies $\Delta E$ (meV/FU) of the $|HS\rangle$, $|BS_1\rangle$ and $|BS_2\rangle$ states of $CdVO_3$ obtained by FP-LAPW calculations

| State | $E$ (Ryd/FU) | $\Delta E$ (meV/FU)[a] |
|---|---|---|
| $|HS\rangle$ | −13542.465395 | 0.0 |
| $|BS_1\rangle$ | −13542.464486 | 12.4 |
| $|BS_2\rangle$ | −13542.464657 | 10.0 |

[a] The $|HS\rangle$ state was taken as the reference.

Table 2
Magnetic moments on V ($\mu_B$/FU) in the $|HS\rangle$, $|BS_1\rangle$ and $|BS_2\rangle$ states of $CdVO_3$ obtained by FP-LAPW calculations[a]

| | $|HS\rangle$ | $|BS_1\rangle$ | | $|BS_2\rangle$ | |
|---|---|---|---|---|---|
| | V | V1 | V2 | V1 | V2 |
| Total | 0.75 | 0.71 | −0.71 | 0.72 | −0.72 |
| $d_{xy}\uparrow$ | 0.62 | 0.62 | 0.05 | 0.63 | 0.05 |
| $d_{xy}\downarrow$ | −0.05 | −0.05 | −0.62 | −0.05 | −0.63 |
| $d_{xz}\uparrow$ | 0.17 | 0.16 | 0.14 | 0.17 | 0.14 |
| $d_{xz}\downarrow$ | −0.14 | −0.14 | −0.16 | −0.14 | −0.17 |
| $d_{yz}\uparrow$ | 0.19 | 0.19 | 0.11 | 0.18 | 0.11 |
| $d_{yz}\downarrow$ | −0.10 | −0.11 | −0.19 | −0.11 | −0.18 |

[a] V1 and V2 refer to the up-spin and down-spin vanadium sites, respectively.

antiferromagnetic states $|BS_1\rangle$ and $|BS_2\rangle$ of $CdVO_3$ (Table 1), in agreement with experiment [4]. Fig. 3 shows the total density of states (DOS) and the partial DOS of the V $3d$ orbitals calculated for the $|HS\rangle$ state. The corresponding DOS plots for the $|BS_1\rangle$ and $|BS_2\rangle$ states of $CdVO_3$ are presented in Figs. 4 and 5, respectively. Our FP-LAPW calculations reveal that approximately 0.7 spin/FU is found on each $V^{4+}$ site, and the spin density of each $V^{4+}$ site resides largely in the $d_{xy}$ orbital (Table 2). These results are consistent with the finding of qualitative electronic structure calculations that the magnetic orbital of a $VO_5$ square pyramid containing a $V^{4+}$ ion is given by the $d_{xy}$ orbital of V that makes $\pi$-antibonding with the $2p$ orbitals of the basal oxygen atoms (Fig. 6) [12, 25].

From Eq. (3a) and the electronic energies of the states $|HS\rangle$ and $|BS_1\rangle$ (Table 1), we obtain $J_e = 24.7$ meV. Using this $J_e$ and the electronic energies of the states $|HS\rangle$, $|BS_1\rangle$ and $|BS_2\rangle$, we obtain $J_c = 7.7$ meV from both Eqs. (3b) and (3c). These values of $J_e$ and $J_c$ are in support of the suggestion by Onoda and Nishiguchi that $J_e$ is ferromagnetic and dominates over $J_c$ in strength [4]. Nevertheless, the calculated $J_e$ value (i.e., 24.7 meV) is larger than the experimental $J$ value (i.e., 8.6 meV) by a factor of approximately 3. However, density functional theory electronic structure calculations tend to overestimate spin exchange parameters. For example, the spin exchange parameters of $A_2MnF_5$ ($A$ = Rb, Cs, $NH_4$, Li) were calculated to be greater than the experimental values by a factor of 3 to 4 [26].



Fig. 3. Plots of the total DOS (solid line) and the partial DOS of the V $3d$ orbitals (dotted line) calculated for the $|HS\rangle$ state of $CdVO_3$ by spin-polarized FP-LAPW calculations.
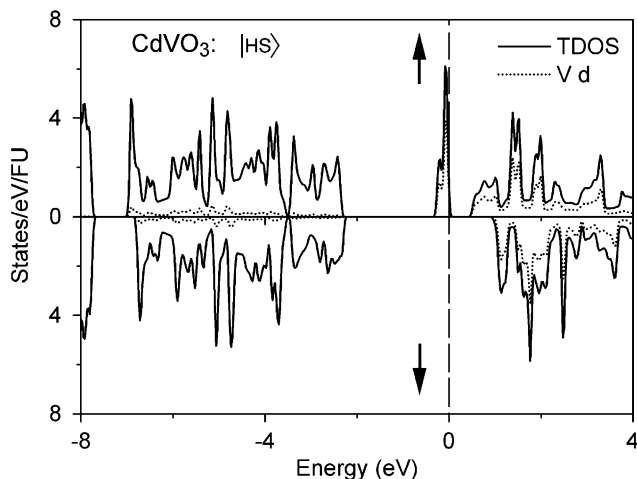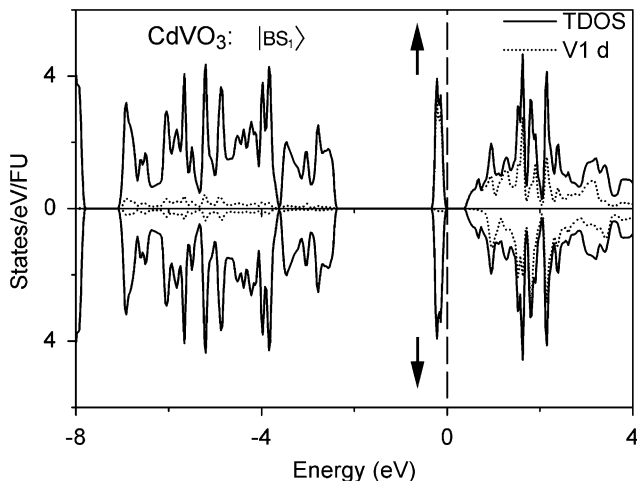


Fig. 4. Plots of the total DOS (solid line) and the partial DOS of the V $3d$ orbitals (dotted line) calculated for the $|BS_1\rangle$ state of $CdVO_3$ by spin-polarized FP-LAPW calculations. Here V1 refers to the vanadium atoms at an up-spin site.

## 4. Qualitative analysis of the spin exchange interactions in $CdVO_3$ and $CaV_2O_5$

In general, a spin exchange parameter $J$ is expressed as $J = J_F + J_{AF}$, where $J_F(>0)$ and $J_{AF}(<0)$ are the ferromagnetic and antiferromagnetic terms, respectively [27,28]. When the two spin sites of a spin dimer are represented by magnetic orbitals $\phi_1$ and $\phi_2$, the ferromagnetic and the antiferromagnetic terms are given by

$$J_F = 2K_{12}, \tag{4a}$$
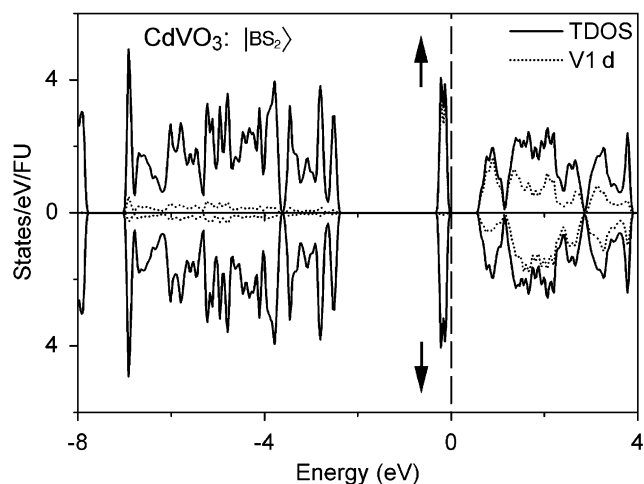
$$J_{AF} = -(\Delta e)^2/U_{eff}, \tag{4b}$$

Fig. 5. Plots of the total DOS (solid line) and the partial DOS of the V $3d$ orbitals (dotted line) calculated for the $|BS_2\rangle$ state of CdVO$_3$ by spin-polarized FP-LAPW calculations. Here V1 refers to the vanadium atoms at an up-spin site.
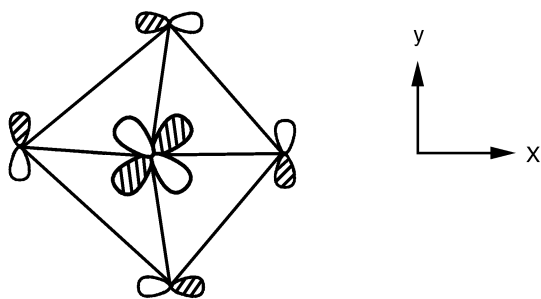


Fig. 6. Magnetic orbital of a VO$_5$ square pyramid containing a V$^{4+}$ ion.

Table 3
Values of $(\Delta e)^2$, $J_{AF}$, $J_{calc}$ and $J_{expt}$ determined for the edge- and corner-sharing spin exchange paths of CdVO$_3$ and CaV$_2$O$_5$[a]

|  |  | $J_e$ | $J_c$ | $J_c'$ |
|---|---|---|---|---|
| CdVO$_3$ | $(\Delta e)^2$ | 1300 | 21000 |  |
|  | $J_{AF}$[b] | −1.3 | −21.7 |  |
|  | $J_{calc}$[c] | 24.7 | 7.7 |  |
| CaV$_2$O$_5$ | $(\Delta e)^2$ | 3800 | 19600 | 50600 |
|  | $J_{AF}$[b] | −3.9 | −20.3 | −52.4 |
|  | $J_{calc}$[d] | 2.4 | −10.5 | −52.4 |
|  | $J_{expt}$[e] | 2.2 | −28.6 | −57.3 |
|  | $J_{expt}$[f] | −3.9 | −5.8 | −57.7 |
|  | $J_{expt}$[g] | −14.6 | −50.6 | −62.9 |

[a] $(\Delta e)^2$ values are given in (meV)$^2$, and $J_{AF}$, $J_{calc}$ and $J_{expt}$ values in meV.
[b] Calculated by using Eq. (4b) with $U_{eff} = 966$ meV.
[c] Calculated from the present FP-APW calculations.
[d] Calculated by the direct method using the LDA + U functional (Ref. [11]).
[e] Deduced from magnetic susceptibility measurements assuming that $J_c/J_c' = 0.2$ (Ref. [10]).
[f] Deduced from magnetic susceptibility measurements assuming that $J_c/J_c' = 0.1$ (Ref. [10]).
[g] Deduced from magnetic susceptibility measurements (Ref. [9]).

where $K_{12}$ is the exchange repulsion between the magnetic orbitals $\phi_1$ and $\phi_2$, and becomes larger with increasing the overlap density distribution $\phi_1\phi_2$ [28]. $U_{eff}$ is the effective on-site repulsion, and $\Delta e$ is the energy separation of the two levels resulting from the interaction between the two magnetic orbitals. In general, $J_F$ is a small positive number so that $J$ becomes ferromagnetic (i.e., $J > 0$) when $J_{AF}$ is negligibly small in magnitude.

The $(\Delta e)^2$ values for the edge- and corner-sharing spin dimers of CdVO$_3$ and CaV$_2$O$_5$ were calculated using the extended Hückel tight binding (EHTB) electronic structure calculations [29,30],[1] as described elsewhere [12,18,25]. Table 3 summarizes the $(\Delta e)^2$ values as well as the corresponding $J_{AF}$ values estimated by using Eq. (4b) with $U_{eff} = 966$ meV, which was chosen to reproduce the $J_c'$ value of CaV$_2$O$_5$ calculated by the direct method [11]. Also listed in Table 3 are the spin exchange parameters determined for CdVO$_3$ and

CaV$_2$O$_5$ from first principles electronic structure calculations ($J_{calc}$), and those derived for CaV$_2$O$_5$ from magnetic susceptibility measurements ($J_{expt}$) [9,10]. In analyzing results of magnetic susceptibility and neutron scattering measurements in terms of spin exchange parameters, the latter become numerical fitting parameters needed to reproduce the experimental results. The nature and values of these "experimental" parameters depend on what spin exchange paths one includes in the analysis and on what constraints one places on them. Thus more than one set of spin exchange parameters can lead to an equally acceptable fitting. The meaningful "experimental" spin exchange parameters for a given magnetic solid are those that are consistent with its electronic structure [12].

Table 3 shows that in CdVO$_3$ the $J_{AF}$ term of the path $J_c$ is significantly larger in magnitude than that of the path $J_e$. This explains why $J_e$ of CdVO$_3$ is more strongly ferromagnetic than $J_c$ of CdVO$_3$ in our quantitative calculations. The $J_{AF}$ term of the path $J_e$ is small in CdVO$_3$ and CaV$_2$O$_5$, so that $J_e$ should be either weakly antiferromagnetic or weakly ferromagnetic. However, the $J_{AF}$ term of the path $J_e$ is considerably smaller in CdVO$_3$ than in CaV$_2$O$_5$, so that the path $J_e$ is likely to be more strongly ferromagnetic in CdVO$_3$. Furthermore, the ferromagnetic terms $J_F$ of the paths $J_e$ and $J_c$ should be greater in CdVO$_3$ than in CaV$_2$O$_5$ for the following reasons: First, $J_e$ is more strongly ferromagnetic in CdVO$_3$ than in CaV$_2$O$_5$. This suggests that CdVO$_3$ has a larger $J_F$ contribution in addition to a negligible $J_{AF}$. Second, the $J_{AF}$ values of the path $J_c$ are similar in CdVO$_3$ and CaV$_2$O$_5$. Nevertheless, $J_c$ is

---
[1] Our calculations were carried out by employing the SAMOA (Structure and Molecular Orbital Analyzer) program package.

weakly ferromagnetic in $CdVO_3$, but substantially antiferromagnetic in $CaV_2O_5$. This implies a greater $J_F$ contribution to the $J_c$ path in $CdVO_3$.

## 5. Geometrical features of spin exchange paths in $CdVO_3$ and $CaV_2O_5$

To see if $CdVO_3$ possesses any structural feature that enhances the $J_F$ term for the exchange paths $J_c$ and $J_e$, we compare the local geometries of the $V^{4+}$ ions in $CdVO_3$ and $CaV_2O_5$. The interatomic distances and bond angles specifying the local structures are defined in Fig. 7 and their values are listed in Table 4. In terms of the $V\cdots V$ and V–O bond lengths as well as the V–O–V and O–V–O bond angles, the local structures of the $V^{4+}$ ions are very similar in $CdVO_3$ and $CaV_2O_5$. A substantial difference between the local structures of $CdVO_3$ and $CaV_2O_5$ lies in the height $\Delta h$ of the $V^{4+}$ ion above the basal plane in each $VO_5$ square pyramid. As can be seen from Fig. 1b, the two $V^{4+}$ ions of each $J_e$ path are located symmetrically on the opposite sides of the "condensed basal plane". Thus the $\Delta h$ value of each $V^{4+}$ ion can be approximated by $\Delta z/2$, where $\Delta z$ is the height difference between the two $V^{4+}$ ions. As listed in Table 4, the $\Delta h$ value is considerably smaller for $CdVO_3$ than for $CaV_2O_5$. Our analysis of the crystal structures of other magnetic solids of $V^{4+}$ ions made up of $VO_5$ square pyramids (e.g., $MgV_2O_5$ [8], $CaV_4O_9$ [31], $SrV_4O_9$ [16], $CdV_3O_7$ [32] and $CaV_3O_7$ [32]) shows that the $\Delta h$ value is smallest for $CdVO_3$. The strength of the $\pi$-interaction between the V $3d_{xy}$ and the basal oxygen $2p$ orbitals (Fig. 6) is enhanced with decreasing the $\Delta h$ value toward zero. An enhancement of the $\pi$-interaction should induce a stronger ferromagnetic term $J_F$ because
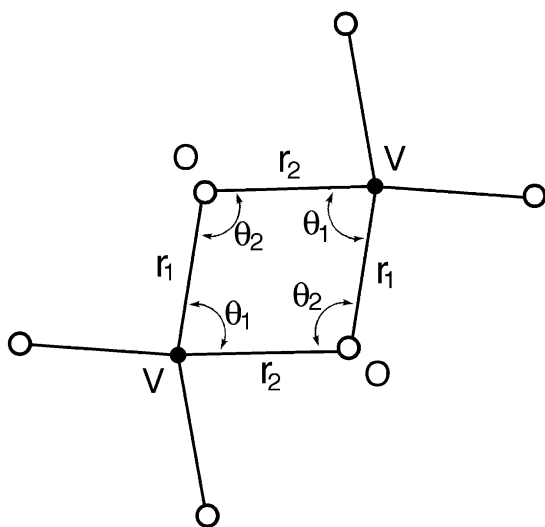
Table 4
Geometrical parameters associated with the $J_e$ paths of $CdVO_3$ and $CaV_2O_5$

|  | $CdVO_3$[a] | $CaV_2O_5$[b] |
|---|---|---|
| $V\cdots V$ (Å) | 3.048 | 3.026 |
| $r_1$ (Å) | 1.940 | 1.949 |
| $r_2$ (Å) | 1.992 | 1.982 |
| $\theta_1$ (°) | 78.4 | 79.4 |
| $\theta_2$ (°) | 101.6 | 100.7 |
| $\Delta h$ (Å) | 0.430 | 0.536 |

[a] Ref. [4].
[b] Ref. [7].

it will increase the overlap density distribution between two magnetic orbitals.

## 6. Concluding remarks

Using first principles spin-polarized FP-LAPW calculations, we estimated the strengths of the spin exchange interactions $J_e$ and $J_c$ in $CdVO_3$. These calculations show that both $J_e$ and $J_c$ are ferromagnetic, but $J_e$ dominates over $J_c$. Our spin dimer analysis based on EHTB electronic structure calculations suggests that in terms of $J_{AF}$ the path $J_e$ is expected to be more strongly ferromagnetic in $CdVO_3$ than in $CaV_2O_5$, and the ferromagnetic terms $J_F$ of the paths $J_e$ and $J_c$ should be greater in $CdVO_3$ than in $CaV_2O_5$. In each $VO_5$ square pyramid, the height of the $V^{4+}$ ion above the basal plane is considerably lower in $CdVO_3$ than in $CaV_2O_5$. This geometrical factor is expected to enhance the $J_F$ term contributions to the spin exchange paths in $CdVO_3$.

Fig. 7. Geometrical parameters defining the local structures around the $V^{4+}$ ions associated with the $J_e$ paths in $CdVO_3$ and $CaV_2O_5$.

## References

[1] J. Galy, J.-C. Bouloux, C. R. Acad. Sci. 264 (1967) 388.
[2] B. Reuter, K. Müller, Z. Anorg. Allg. Chem. 368 (1969) 174.
[3] B.L. Chamberland, P.S. Danielson, J. Solid State Chem. 10 (1974) 249.
[4] M. Onoda, N. Nishiguchi, J. Phys.: Condens. Matter 11 (1999) 749.
[5] M.E. Fischer, Am. J. Phys. 32 (1964) 343.

[6] J.B. Goodenough, Magnetism and the Chemical Bond, Interscience, New York, 1963 (Chapter 3).

[7] M. Onoda, N. Nishiguchi, J. Solid State Chem. 127 (1996) 359.

[8] M. Onoda, A. Ohyama, J. Phys.: Condens. Matter 10 (1998) 1229.

[9] Y. Ueda, Chem. Mater. 10 (1998) 2653.

[10] S. Miyahara, M. Troyer, D.C. Johnston, K. Ueda, J. Phys. Soc. Jpn. 67 (1998) 3918.

[11] M.A. Korotin, V.I. Anisimov, T. Saha-Dasgupta, I. Dasgupta, J. Phys.: Condens. Matter 12 (2000) 113.

[12] M.-H. Whangbo, H.-J. Koo, D. Dai, J. Solid State Chem., in press.

[13] G. Liu, J.E. Greedan, J. Solid State Chem. 115 (1995) 174.

[14] K. Kodama, H. Harashina, H. Sasaki, Y. Kobayashi, M. Kasai, S. Taniguchi, Y. Yasui, M. Sato, K. Kakurai, T. Mori, M. Nishi, J. Phys. Soc. Jpn. 66 (1997) 793.

[15] Y. Fukumoto, A. Oguchi, J. Phys. Soc. Jpn. 67 (1998) 2205.

[16] Y. Oka, T. Yao, N. Yamamoto, M. Ueda, S. Maegawa, J. Solid State Chem. 149 (2000) 414.

[17] Y. Zhang, C.J. Warren, R.C. Haushalter, A. Clearfield, D.-K. Seo, M.-H. Whangbo, Chem. Mater. 10 (1998) 1059.

[18] H.-J. Koo, M.-H. Whangbo, J. Solid State Chem. 153 (2000) 263.

[19] For a recent review, see: F. Illas, I. de P. R. Moreira, C. de Graaf, V. Barone, Theor. Chem. Acc. 104 (2000) 265.

[20] D. Dai, M.-H. Whangbo, J. Chem. Phys. 118 (2003) 29.

[21] A. Chartier, P. D'Arco, R. Dovesi, V.R. Saunders, Phys. Rev. B 60 (1999) 14042 and the references cited therein.

[22] A.I. Liechtenstein, V.I. Anisimov, J. Zaanen, Phys. Rev. B 52 (1995) R5467.

[23] P. Blaha, K. Schwarz, G. Madsen, D. Kvasnicka, J. Luitz, WIEN2k, An Augmented Plane Wave + Local Orbitals Program for Calculating Crystal Properties, Karlheinz Schwarz, Techn. Universität Wien, Austria, 2001. ISBN 3-9501031-1-2. See also: http://www.wien2k.at/

[24] J.P. Perdew, S. Burke, M. Ernzerhof, Phys. Rev. Lett. 77 (1996) 3865.

[25] H.-J. Koo, M.-H. Whangbo, Inorg. Chem. 39 (2000) 3599.

[26] D. Dai, M.-H. Whangbo, J. Chem. Phys. 114 (2001) 2887.

[27] P.J. Hay, J.C. Thibeault, R. Hoffmann, J. Am. Chem. Soc. 97 (1975) 4884.

[28] O. Kahn, Molecular Magnetism, VCH Publishers, Weinheim, 1993.

[29] R. Hoffmann, J. Chem. Phys. 39 (1963) 1397.

[30] D. Dai, J. Ren, W. Liang, M.-H. Whangbo, http://chvamw.chem.ncsu.edu.

[31] J.C. Bouloux, J. Galy, Acta Crystallogr. B 29 (1973) 1335.

[32] N. Nishiguchi, M. Onoda, K. Kubo, J. Phys.: Condens. Matter 14 (2002) 5731.